

Nuclear Pore Complex Is Able to Transport Macromolecules with Diameters of ~ 39 nm

Nelly Panté*^{†‡} and Michael Kann[§]

*Swiss Federal Institute of Technology Zurich, Institute of Biochemistry, CH-8092 Zurich, Switzerland; and [§]Institute of Medical Virology, Justus Liebig University, D-35392 Giessen, Germany

Submitted June 22, 2001; Revised October 26, 2001; Accepted November 21, 2001
Monitoring Editor: Pamela A. Silver

Bidirectional transport of macromolecules between the nucleus and the cytoplasm occurs through the nuclear pore complexes (NPCs) by a signal-mediated mechanism that is directed by targeting signals (NLSs) residing on the transported molecules or “cargoes.” Nuclear transport starts after interaction of the targeting signal with soluble cellular receptors. After the formation of the cargo-receptor complex in the cytosol, this complex crosses the NPC. Herein, we use gold particles of various sizes coated with cargo-receptor complexes to determine precisely how large macromolecules crossing the NPC by the signal-mediated transport mechanism could be. We found that cargo-receptor-gold complexes with diameter close to 39 nm could be translocated by the NPC. This implies that macromolecules much larger than the assumed functional NPC diameter of 26 nm can be transported into the karyoplasm. The physiological relevance of this finding was supported by the observation that intact nucleocapsids of human hepatitis B virus with diameters of 32 and 36 nm are able to cross the nuclear pore without disassembly.

INTRODUCTION

Bidirectional transport of macromolecules between the nucleus and the cytoplasm is a major and essential activity in eucaryotic cells. The double nuclear membrane, which separates the nucleoplasm from the rest of the cell, contains specialized channels called nuclear pore complexes (NPCs) through which nuclear import and export occur (reviewed by Mattaj and Englmeier, 1998; Nakielny and Dreyfuss, 1999; Wente 2000). NPCs allow passive diffusion of ions and small molecules through aqueous channels with a diameter of ~ 9 nm (Paine *et al.*, 1975). Molecules larger than this diffusion limit are selectively transported in and out of the nucleus by a signal-mediated process (De Robertis *et al.*, 1978; Dingwall *et al.*, 1982). Signals mediating import of nuclear proteins (called nuclear localization sequences or NLSs) were identified more than two decades ago (Dingwall *et al.*, 1982). Early studies in cells injected with various sizes of gold particles coated with the NLS-bearing protein nucleoplasmin showed that the NPC can import NLS-coated

gold particles that are up to ~ 26 nm in diameter (including the protein coat; Dworetzky *et al.*, 1988), which resulted in the general belief that this diameter reflects the threshold size for karyophilic macromolecules crossing the NPC. More recently, it has been shown that the NLSs on the macromolecule or “cargo” to be transported are recognized by soluble receptor proteins, and that the cargo-receptor complex crosses the NPC (Görlich *et al.*, 1994, 1995; Moroianu *et al.*, 1995; Radu *et al.*, 1995). Therefore, it is expected that after cytoplasmic injection of NLS-coated gold particles into cells, the NLS-coated gold particles will be modified by the binding of intracellular import receptors to the NLSs. Consistent with this, the interaction between the two receptors, termed importin (karyopherin) α and β , for classical NLSs, was speculated to increase the diameter of the transported complex by ~ 8 nm (Ribbeck and Görlich, 2001).

The knowledge of the exact functional diameter of the NPC is very important in the field of virology. Many viruses that infect eucaryotic cells replicate in the nucleus. During infection, these viruses have to cross the NPC. This is achieved by mimicking cellular NLSs and by using the cellular import receptors to cross the NPC (reviewed by Kasamatsu and Nakanishi, 1998; Whittaker and Helenius, 1998; Whittaker *et al.*, 2000). However, based on the previous reported value for the functional diameter of the NPC (Dworetzky *et al.*, 1988), it has been assumed that viruses >26 nm have to disassemble into small components before they cross the NPC. For example, because the genome-containing nucleocapsids of hepatitis B viruses (HBVs) (also termed cores), which replicate their viral DNA inside the

Article published online ahead of print. Mol. Biol. Cell 10.1091/mbc.01-06-0308. Article and publication date are at www.molbiol-cell.org/cgi/doi/10.1091/mbc01-06-0308.

[†] Present address: Department of Zoology, University of British Columbia, 6270 University Blvd., Vancouver, British Columbia V6T 1Z4, Canada.

[‡] Corresponding author. E-mail address: pante@zoology.ubc.ca. Abbreviations used: BSA, bovine serum albumin; EM, electron microscopy; HBV, hepatitis B virus; NLS, nuclear localization sequence; NP, nucleoplasmin; NPC, nuclear pore complex.

nucleus of the infected cell, have diameters of 32 or 36 nm (dependent upon their symmetry; Crowther *et al.*, 1994; Kenney *et al.*, 1995), it has been assumed that they are too big to cross the NPC without disassembly. Thus, the current hypothesis by which HBV delivers its genome into the cell nucleus is that the core particles disassemble at the cytoplasmic face of the NPCs where a complex of viral DNA and covalently bound polymerase is released, followed by the nuclear import of the genome, mediated by the viral polymerase (Kann *et al.*, 1997). These assumptions are thought to be true not only for the initial infection of the cell but also for the delivery of progeny genomes from the cytosol into the already infected nucleus, which amplifies nuclear viral DNA leading to persistent infection on the cellular level. Consistent with this model, it has been shown by indirect immunofluorescence microscopy that *Escherichia coli*-grown HBV cores bind to the NPCs of digitonin-permeabilized cells without migration into the free karyoplasm (Kann *et al.*, 1999). These recombinant HBV core particles, used by Kann *et al.* (1999), are morphologically and immunologically identical to authentic virus-derived core particles (Kenney *et al.*, 1995). However, in contrast to authentic cores, they do not contain either the viral DNA or the polymerase, but bacterial RNA. Kann *et al.* (1999) have also shown that the *E. coli*-expressed HBV core particles only bind to the NPC of permeabilized cells when they are phosphorylated, and that NPC binding is also mediated by importin α and β . Because these studies by indirect immunofluorescence microscopy lack the resolution necessary to visualize the docking of the HBV cores to single nuclear pores, electron microscopy (EM) studies of the NPC docking of HBV cores are necessary to identify where at the NPC the core particle disassemble and what is the strategy followed by HBV to release its genome into the cell nucleus.

In the present study we have structurally characterized cargo-receptor-coated gold particles and used them in import assays to directly determine the functional diameter of the NPC. We found that cargo-receptor-gold complexes as large as 39 nm in diameter (including the cargo-receptor coat) can be imported into the nucleus by the NLS-mediated transport mechanism. To show the physiological relevance of our findings we then studied nuclear import of human HBV nucleocapsids. Consistent with our results with cargo-receptor-gold complexes we found that intact HBV capsids with diameters of 32 and 36 nm are able to cross the NPC without disassembly.

MATERIALS AND METHODS

Gold Particles and Protein-Gold Complexes

Colloidal gold particles with diameter of 22 ± 2 , 26 ± 3 , and 36 ± 4 nm were prepared by reduction of tetrachloroauric acid with sodium citrate (Frens, 1973). Nucleoplasmin (NP) was kindly provided by Dr. Dirk Görlich, Zentrum für Molekulare Biologie der Universität Heidelberg, University of Heidelberg, Germany.

Gold particles were coated with NP or bovine serum albumin (BSA; Sigma, St. Louis, MO) according to Baschong and Wrigley (1990) with some modifications. Namely, protein was added to the colloidal gold solution, while stirring, to an amount that exceeded 10 times the minimal stabilization amount to ensure that the gold particles were fully stabilized and would not increase their coat size by attracting nonspecific proteins upon injection into cells. The protein-gold complexes were then centrifuged at $45,000 \times g$ for 15

min, and the soft pellet was resuspended in low-salt buffer (LSB; 1 mM KCl, 0.5 mM MgCl₂, 10 mM HEPES, pH 7.5) and used immediately for microinjection.

To form the NP-receptor-gold complex, both NP- and BSA-coated gold particles were incubated at 4°C for 2 h with an excess of importin α . The gold complexes were centrifuged at $45,000 \times g$ for 15 min and the soft pellet was resuspended in LSB. The importin α -incubated gold complexes were further incubated at 4°C for 2 h with an excess of importin β . The resulting gold complexes were centrifuged at $45,000 \times g$ for 15 min, and the soft pellet was resuspended in LSB and used immediately for microinjection.

Negative Staining

To measure the size of the protein coat of the gold-protein complexes, these were negatively stained and examined in the electron microscope. For this purpose, the gold-protein complexes were adsorbed for 2 min onto glow-discharged carbon-coated palladium films on copper EM grids. The grids were then washed on 3 drops of LSB before they were negatively stained with 0.75% uranyl formate for 1 min.

Immunogold Labeling

For immunogold labeling, colloidal gold particles, ~8 nm in diameter, were prepared as described (Slot and Geuze, 1985), and an anti-importin β antibody was conjugated to the colloidal gold particles as described (Baschong and Wrigley, 1990). The importin α - and β -incubated gold particles were adsorbed for 2 min onto glow-discharged carbon-coated palladium films on copper electron microscopy grids, and the grids were incubated with the gold-coupled antibody for 1 h at room temperature. After incubation, the grids were washed on three drops of LSB and were negatively stained with 0.75% uranyl formate for 1 min.

HBV Core Particles

HBV core particles were obtained from G. Borisova and P. Pumpens (Biomedical Research and Study Center, Riga, Latvia) and phosphorylated according to Kann and Gerlich (1994).

Electron Microscopy Import Assay in *Xenopus laevis* Oocytes

Mature (stage 6) oocytes were surgically removed from *X. laevis* as described previously (Panté *et al.*, 1997). Fresh-made gold-protein complexes (~50 nl) or HBV core particles were microinjected into the cytoplasm of the oocytes. Injected oocytes were then incubated at room temperature in modified Barth's saline buffer [88 mM NaCl, 1 mM KCl, 0.82 mM MgSO₄, 0.33 mM Ca(NO₃)₂, 0.41 mM CaCl₂, 10 mM HEPES, pH 7.5] for 1 h (NP-injected oocytes) or 15–30 min (HBV-injected oocytes). The oocytes were prepared for embedding in Epon 812 resin (Fluka, Buchs, Switzerland) as described by Panté *et al.* (1997). Ultrathin sections were collected on palladium/carbon-coated copper EM grids and were stained by conventional procedures (Panté *et al.*, 1997).

Electron Microscopy and Quantitation

All micrographs were digitally recorded in a Hitachi H-7000 transmission electron microscope (Hitachi, Tokyo, Japan) operated at an acceleration voltage of 100 kV. Magnification calibration was performed as described (Wrigley, 1968).

The sizes of the gold particles and their protein coats were determined from digital electron micrographs of negatively stained preparations by using Adobe Photoshop 5.5 (Adobe Systems, Mountain View, CA). The diameter of gold particles in the nucleus of injected *Xenopus* oocytes and HBV core particles was determined from dig-

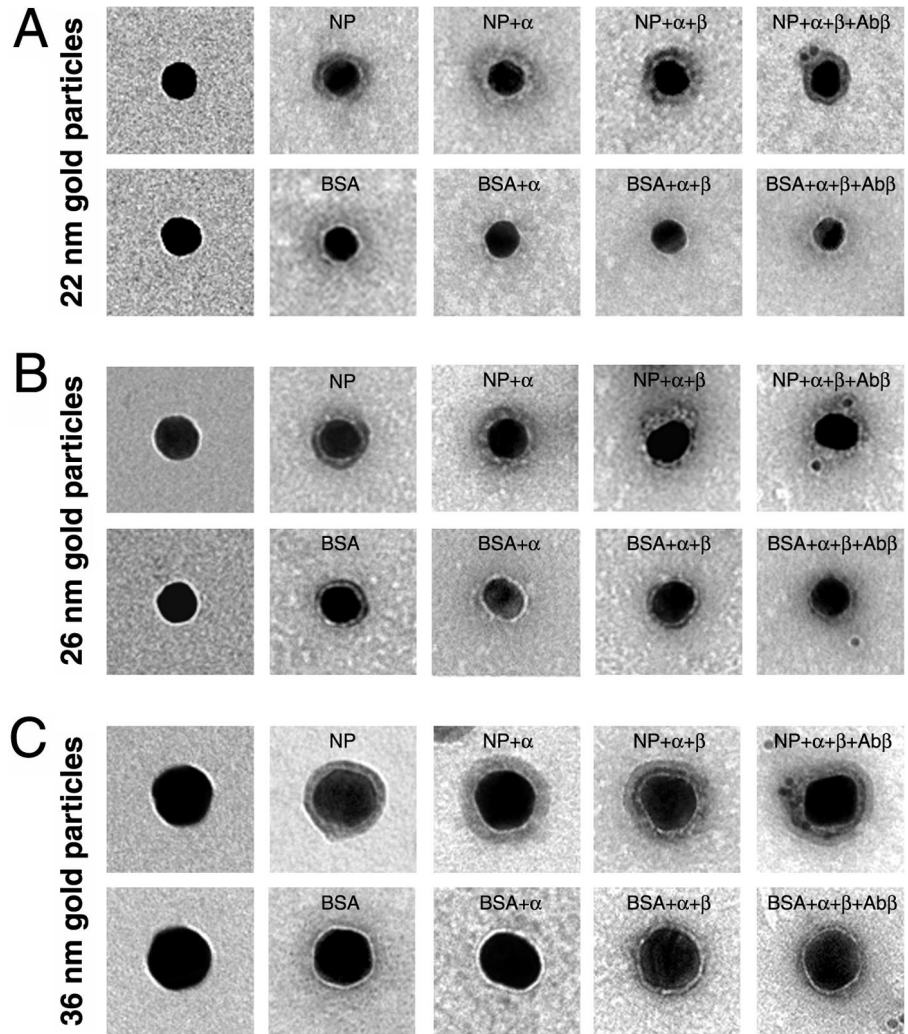


Figure 1. Electron microscopy of representative gold particles and their protein coat. Gold particles (A, 22 nm; B, 26 nm; and C, 36 nm) uncoated (first row) and coated with NP or BSA (second row) were visualized in the electron microscope by negative staining. The third and fourth rows are examples of NP- and BSA-coated gold particles that were incubated first with importin α (NP + α and BSA + α) and then with importin β (NP + α + β and BSA + α + β). The last row shows examples of NP- and BSA-coated gold particles that were incubated with importin α and β and then immunogold labeled with an anti-importin β antibody directly conjugated with 8-nm gold particles.

ital electron micrographs revealing cross sections of NPCs along the nuclear envelope.

RESULTS

Cargo-Receptor Coat Can Add an Additional 13 nm to Diameter of Gold Particles

To determine precisely how large macromolecules crossing the NPC by the signal-mediated transport mechanism could be, we coated gold particles of various sizes with import cargoes and their import receptors and determined the exact size of the cargo-receptor coat by high-resolution electron microscopy. For these experiments we used nucleoplasmin (a nuclear protein from *X. laevis* oocytes containing two classical NLSs of basic amino acids), and the receptor for classical NLS, which consists of two functionally different subunits (importin [karyopherin] α and β). As illustrated in Figure 1 (also Table 1), for gold particles of 22–36 nm in diameter, the protein coating contributed to a low-density layer that surrounds the gold particles, which was revealed by contrasting the protein-gold complexes with uranyl for-

mate (i.e., by negative staining). Whereas the thickness of this layer was only ~ 4 nm on each side (Table 1) when the protein coat consisted of BSA, this layer was 6.6 nm in average (5.2–8.3 nm/side) for NP, reflecting the different molecular mass of BSA (68 kDa) and NP (165 kDa). The observed protein layers are in the same order of the protein layer of concanavalin A (108 kDa), which is a 4×8 -nm molecule and yielded gold particles with a 4-nm coat (Horisberger and Rosset, 1977). However, it must be considered that the interactions of proteins and colloidal gold depend not only on the molecular mass of the protein but also on a combination of many factors, including shape, electrical charge, and hydrophobic properties of the protein.

As we expected, when these NP-coated gold particles were incubated in vitro with importin α , the association of importin α to the NLSs of NP-coated gold particles increased the protein layer around the gold particles by 1.3–3 nm (on average) per radius (Figure 1, row 3; and Table 1). In contrast, the protein coat of the gold particles remained more or less constant for BSA-coated gold particles that were incubated in vitro with importin α (Figure 1 and Table 1).

Table 1. Thickness of the protein coat (nm) surrounding the gold particles

| | Protein | Protein + importin α | Protein + $\alpha + \beta$ |
|--------------------|--|-----------------------------|------------------------------|
| 22 \pm 2 nm gold | | | |
| NP | 6.5 \pm 0.8 ^a (5.2–8.3) ^b | 7.8 \pm 2.1 (5.2–13.6) | 8.4 \pm 1.8 (5.2–13.6) |
| BSA | 3.6 \pm 0.3 (3.1–4.1) | 3.6 \pm 0.5 (3.1–4.2) | 3.7 \pm 0.5 (3.1–4.2) |
| 26 \pm 3 nm gold | | | |
| NP | 6.6 \pm 0.9 (5.2–8.3) | 8.1 \pm 1.8 (5.2–10.4) | 8.5 \pm 1.5 (5.2–9.4) |
| BSA | 4.2 \pm 0.4 (3.1–5.2) | 4.2 \pm 0.5 (3.1–5.2) | 3.9 \pm 0.5 (3.1–5.2) |
| 36 \pm 4 nm gold | | | |
| NP | 6.9 \pm 0.7 (6.3–8.3) | 9.9 \pm 1.8 (7.3–13.6) | 10.2 \pm 1.7 (7.3–12.5) |
| BSA | 3.9 \pm 0.5 (3.1–5.2) | 4.4 \pm 0.5 (3.1–5.2) | 4.2 \pm 0.4 (3.1–5.2) |

^a Average \pm standard deviation.

^b Minimum and maximum coat. The minimum and maximum sizes of the protein coat from 20 gold particles were analyzed for each state.

The NP-importin α layer that surrounded the gold particles was less compact than the NP layer, and varied in thickness even on the same gold particle (which is reflected in the large values for the SD). This variability was expected in agreement with the random adsorption of NP onto the surface of the gold particles. In addition, the size of the NP-importin α was predicted from the geometry of importin α and the way it accommodates the NLSs of NP. Importin α is an elongated molecule with a cylindrical shape of 10 \times 3 nm and can accommodate the bipartite NLS of NP within the center of the molecule (Conti *et al.*, 1998). The two NLS-binding sites are located at \sim 2 and 3 nm from each end of the molecule. Thus, if the binding of importin α to the NP-coated gold particles is in a “side-on” orientation, $<$ 2 nm (i.e., the radius of the cylindrical molecule) will be added to the NP-layer per side. On the other hand, if importin α is added in an end-on orientation most of the importin α molecule will be embedded on the NP coat and only 2 or 3 nm from the importin α molecule will be added to the previous NP coat.

As illustrated (Figure 1, row 4; Table 1), when these gold-NP-importin α complexes were incubated in vitro with importin β , the binding of importin β to importin α on these gold particles contributed an additional 0.3–0.6 nm in average to the protein layer per radius. This low increment in the protein coat was expected because when importin β interacts with the importin β -binding domain of importin α , it is embedded within the structure of importin β (Cingolani *et al.*, 1999). Again, there was no increase in the thickness of the protein layer in the control experiments with BSA-coated gold particles that were incubated in vitro first with importin α and then with importin β . Similar to the gold-NP-importin α complex, the gold-NP-importin α - β complex has a very heterogeneous protein coat (Figure 1, row 4), which is a consequence of the irregular coat from the gold-NP-importin α particles. Taken together, these results indicate that

the incorporation of importin α and β into NP-coated gold particles increased the protein coat by 1.9–3.3 nm/radius on average. However, in some cases the total NP-importin α and β layer was as large as 13.6 nm (Table 1).

To obtain further evidence of the extra layer contributed by the two subunits of the import receptor, we used an anti-importin β antibody conjugated with 8-nm-diameter gold particles to locate importin β within the gold-NP-receptor complex. As shown in Figure 1, this antibody labeled the NP-coated gold particles that were incubated with importin α and importin β , but not BSA-coated gold particles that were also incubated with importin α and importin β . For the gold-NP- α - β complex, the distance between the large gold particle (coated with NP) and the 8-nm antibody-coupled gold particle was 8–10 nm. These values agree with the thickness of the cargo-receptor layer that surrounds the gold particles as measured after negative staining (Figure 1 and Table 1).

Nuclear Import of Large NP-coated Gold Particles

Our results of the thickness of the protein coat surrounding NP-receptor-coated gold particles clearly document that the binding of importin α and importin β to the NP-coated gold particles increase the diameter of the protein-gold complexes. Because the protein coat surrounding the gold particle cannot be resolved in electron micrographs of plastic-embedded and sectioned cells, it is very important to know precisely the exact size of the protein coat that surrounds the gold particle before they are injected into cells. To accurately determine the functional diameter of the NPC, we microinjected our NP-gold particles (of known protein coat; Figure 1) into the cytoplasm of *Xenopus* oocytes, and followed their fate by electron microscopy. As demonstrated previously (Feldherr *et al.*, 1984; Richardson *et al.*, 1988; Panté *et al.*, 1996), NP-coated gold particles were targeted to the NPCs and, depending on the size of the gold particles, were imported into the nucleus (Figure 2). In contrast, BSA-coated gold particles remained in the cytoplasm. We found that 1 h after injection, 36% of NP-gold particles with diameter of 22 \pm 2 nm (without the NP coat) were imported into the nuclei of *Xenopus* oocytes (Figures 2A and 3A and Table 2). Similarly, 28% of NP-gold particles with diameter of 26 \pm 3 nm reached the *Xenopus* nuclei (Figures 2B and 3B and Table 2). In contrast, NP-gold particles with diameter of 36 \pm 4 nm were excluded from the nucleus of *Xenopus* oocytes. However, these last particles were able to associate with the cytoplasmic face of the NPC (Figure 2C). The difference in the efficiency of nuclear import for gold particles of 22 \pm 2 and 26 \pm 3 nm in diameter is consistent with the notion that large particles diffuse more slowly through the cytoplasm than small particles. Thereby, at any given time after injection more gold particles reached the NPCs in oocytes injected with 22-nm NP-gold than in those injected with 26-nm NP-gold particles.

For gold particles $>$ 20 nm in diameter it is very difficult to obtain particles that are homogeneous in size (Slot and Geuze, 1985). This is reflected in the large SD of the diameter of the gold particles used in this study. For example, the 22-nm gold particle preparation contained particles with diameters from 15 to 26 nm; the 26-nm preparation consisted of particles ranging from 19 to 34 nm (Figure 3, A and B). Thus, we could not exclude that only the smaller particles of this gold preparation entered the nucleus.

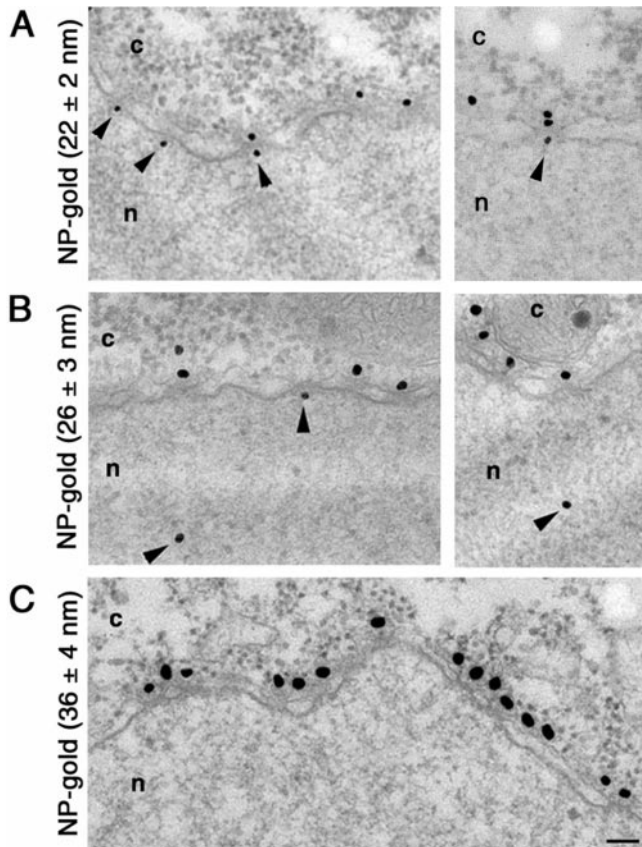


Figure 2. Nuclear import of NP-coated gold particles into *Xenopus* oocyte nuclei. Gold particles of 22 ± 2 nm (A), 26 ± 3 nm (B), and 36 ± 4 nm (C) in diameter were coated with NP and their nuclear import was followed by electron microscopy 1 h after injection into the cytoplasm of *Xenopus* oocytes. Shown are views of nuclear envelope cross sections with adjacent cytoplasm (c) and nucleoplasm (n). Arrowheads point to gold particles that reached the nucleus or are associated with the nuclear face of the NPC. Gold particles 28 nm in diameter or smaller (without the protein coat) were imported into the nucleus. Bar, 100 nm.

Therefore, to determine exactly the maximum size of the NP-gold complexes crossing the NPC, we then measured the diameter of those gold particles that reached the nucleus and compared their distribution with those available for

nuclear import (i.e., distribution of the particle sizes in the cytoplasm and in the preparations). As shown in Figure 3A, by using the 22-nm NP-gold particle preparation, all gold sizes from 15 to 26 nm were able to enter the nucleus. In accordance, the size distribution was the same for particles in the nucleus, the cytoplasm, and the total available particles (Figure 3A). In contrast, in our NP-gold preparation with an average size of 26 nm, which contained gold particles from 19 to 34 nm, mainly particles 26 nm in diameter or smaller reached the nucleus (Figure 3B) with a low percentage of larger particles, showing a diameter of 28 nm. This resulted in a different size distribution for total, nuclear, and cytoplasmic gold particles and most likely indicated a size limit of the NPC.

To calculate the functional diameter of the NPC, we then considered that these 28-nm NP-gold particles were coated with a protein layer of the minimal size (5.2 nm/radius). Our results indicate that the gated channel, located in the center of the NPC through which macromolecule transport occurs, is able to accommodate NLS-bearing macromolecules as large as 38.4 nm in diameter (28 nm gold + 2×5.2 -nm protein coat). A more statistical estimation will be taking the size of gold particles that are most frequently found in the nucleus and the average of the NP layer. This will result in a NPC functional diameter that is ~ 39 nm (26 nm gold + 2×6.6 -nm protein coat).

Nuclear Import of NP-Importin α - β -coated Gold Particles

However, it cannot be concluded from the above-mentioned experiments, how many receptor molecules were actually bound by the NP-gold particles during their time within the cytoplasm. The particles might have bound just some molecules, which would not have a significant impact on the size of the complex that passes the nuclear pore, or they might have acquired an entire additional protein shell of importin α and β . Because EM cannot solve the possible variation in the size of the protein coat (see gallery of gold particles in Figure 4B), we incubated our NP-coated gold particles with importin α and importin β (i.e., the gold-NP- α - β complexes, which have a protein coat of 8.5 ± 1.5 nm; Figure 1 and Table 1), and used these in nuclear import assays in *Xenopus* oocytes.

Similar to the results with NP-coated gold particles, we found that gold-NP- α - β complexes with gold particles of 22 ± 2 , 26 ± 3 , and 36 ± 4 nm in diameter were targeted to

Table 2. Nuclear import of NP- and NP-receptor-coated gold particles

| Size of gold particles (nm) ^a | Protein coat | Nuclear gold (%) | N/C gold ratio | Total no. of gold particles measured |
|--|-------------------------|------------------|----------------|--------------------------------------|
| 22 ± 2 | NP | 35.8 | 0.56 | 300 |
| | NP + α + β | 35.0 | 0.54 | 278 |
| 26 ± 3 | NP | 28.4 | 0.40 | 276 |
| | NP + α + β | 28.7 | 0.40 | 288 |
| 36 ± 4 | NP | 0 | 0 | 100 |
| | NP + α + β | 0 | 0 | 100 |

^a Average \pm standard deviation. Four oocytes were analyzed for each condition.

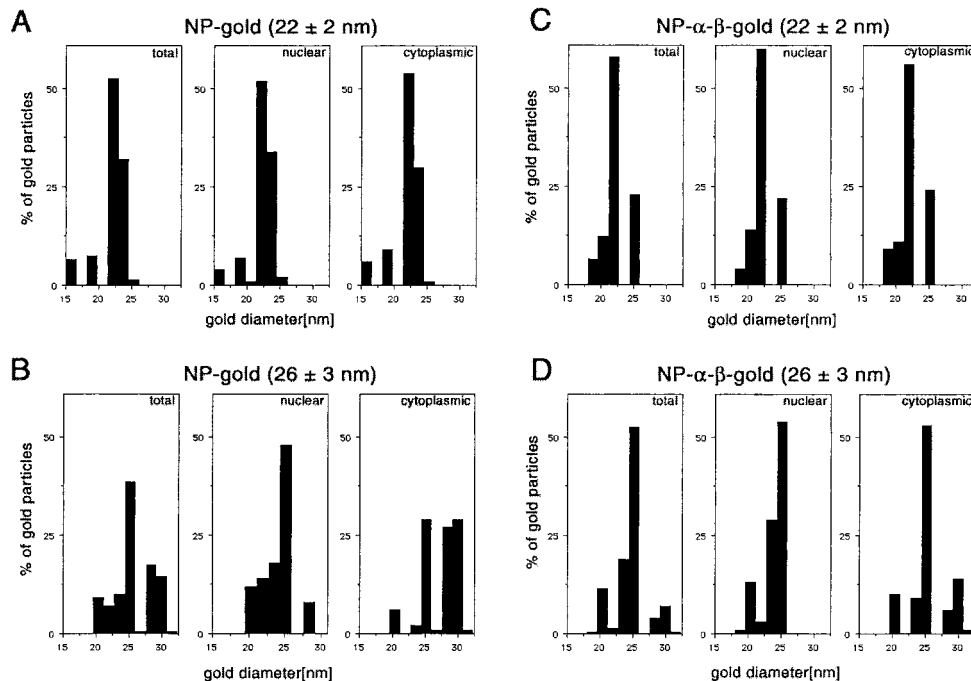


Figure 3. Histograms on the size distribution of gold particles available for import (total), and found within the cytoplasm and the nucleus. Twenty-two ± 2 nm-gold particles, coated with NP (A), 26 ± 3 nm-gold particles, coated with NP (B), 22 ± 2 nm-gold particles, coated with NP and importin α and β (C), and 26 ± 3 nm-gold particles, coated with NP and importin α and β (D). For comparison, only 100 particles in the nucleus and 100 particles in the cytoplasm were measured. The data were derived from microinjections in four different oocytes.

the cytoplasmic face of the NPC and were imported into the nucleus, depending upon the size. As documented in Table 2, the efficiency of nuclear import of NP-α-β-coated gold particles was comparable with that of NP-gold for both the 22 ± 2- and the 26 ± 3-nm gold preparations.

Similar to the NP-coated gold particles from the 22-nm preparation (Figure 3A), the size distribution of total, nuclear, and cytoplasmic particles was identical for the 22-nm preparation, coated with NP, importin α and β (Figure 3C). Using the 26-nm preparation, in which gold particles of 19–34 nm in diameter were available for import, different distribution between nuclear and cytoplasmic gold was observed (Figure 3D); a difference similar to that obtained for the NP-coated 26-nm preparation (Figure 3B). However, the threshold for the NP-α-β-gold was 26 nm in diameter. Although there were less gold parti-

cles with diameter larger than 26 nm in the NP-α-β-gold preparation than in the NP-gold preparation, the divergent threshold for just NP-coated gold particles and the importin α + β + NP-coated gold particles indicates a size difference of ~2 nm, perfectly reflecting the additional average protein coat of importin α and β of 1.9 nm as shown in Table 1. This divergence supports the concept that after injection of the gold-NP-α-β complex the protein layer does not dissociate before the import through the NPC. However, the diameter of the most frequently imported gold-NP-α-β complexes was 26 nm, as for the just NP-coated particles. This result is in accordance with the high variability of the importin α/β coat, explaining that a large proportion of just NP-coated gold particles have the same size, than gold particles coated with importin α and β additionally.

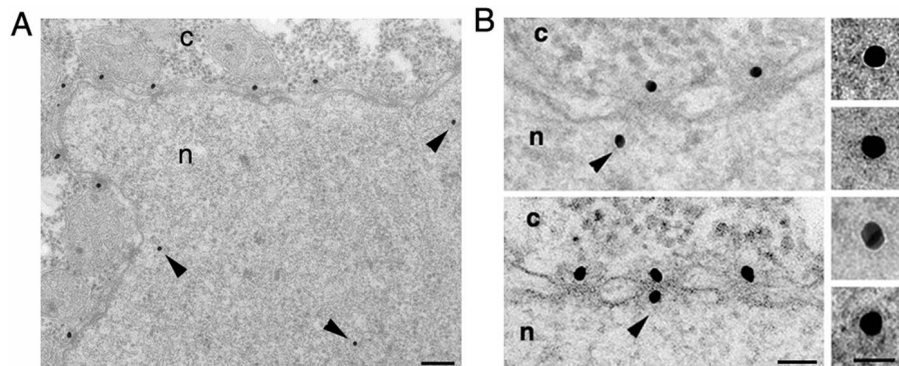


Figure 4. Nuclear import of NP-importin α- and β-coated gold particles into *Xenopus* oocyte nuclei. NP-coated gold particles with diameter of 26 ± 3 nm were incubated in vitro first with importin α and then with importin β. The resulting complexes were injected into the cytoplasm of *Xenopus* oocytes and their nuclear import was followed by electron microscopy. Shown are low- (A) and high (B)-magnification views of nuclear envelope cross sections with adjacent cytoplasm (c) and nucleoplasm (n). Arrowheads point to gold particles that reached the nucleus or are associated with the nuclear face of the NPC. Gold particles as

large as 26 nm in diameter (without the protein coat) were able to cross the nuclear pores and enter the nucleus of *Xenopus* oocytes. Shown is also a gallery of gold particles that were found in the nucleus of *Xenopus* oocytes. Bars, 200 nm (A) and 50 nm (B).

Nuclear Import of Intact Hepatitis B Virus Cores

To verify the functional diameter of the NPC as well as to show the physiological relevance of this observation we then injected viral capsids in our *Xenopus* import assay. We chose nucleocapsids (also termed cores) from HBV, a virus capsid that exceeds the size of the previously reported functional diameter of the NPC and therefore were assumed not to cross the NPCs. Similar to the immunofluorescence microscopy studies reported by Kann *et al.* (1999), we used *E. coli*-expressed core particles that do not disintegrate at the NPC, as shown by using a particle-specific antibody (Kann *et al.*, 1999). For these experiments we first generated phosphorylated recombinant HBV (P-rHBV) cores (unphosphorylated cores do not bind to the NPC; Kann *et al.*, 1999), injected them into the cytoplasm of *Xenopus* oocytes, and followed their nuclear import by electron microscopy. As we expected, the P-rHBV cores, but not the unphosphorylated rHBV cores, were targeted to and bound by *Xenopus* NPCs. According to our size determination of the functional diameter of the NPC, but in contrast to the current theory of HBV genome import, we found intact P-rHBV cores lined up inside the central channel of the NPCs and associated with the nuclear side of the NPCs (Figure 5A) but not in the free karyoplasm. The diameter of the P-rHBV cores found in the center of the NPCs and the diameter of those cores that reached the nuclear side of the NPCs were the same as the diameter of the cores found in the cytoplasm or associated with the cytoplasmic face of the NPCs (Figure 5B). The results of these experiments clearly shown that the 32- and 36-nm diameter P-rHBV cores are able to cross the NPC. Thus, and in accordance with previously published data (Kann *et al.*, 1999), these NPC-associated core particles did not disassemble, but remained intact while crossing the NPC.

DISCUSSION

In this study we used gold particles coated with cargo-receptor complexes in combination with import assays in *Xenopus* oocytes and high-resolution electron microscopy to determine the maximum size that macromolecules crossing the NPC by the signal-mediated transport mechanism could be. As the protein coat surrounding the gold particle cannot be resolved in embedding and thin section, we first measured the exact size of the protein coat that surrounds the gold particle before they were used for import assays.

Our results of nuclear import of nucleoplasmin-coated gold particles indicate that using a preparation with particles from 19 to 34 nm in diameter, nearly 50% of the nuclear gold particles showed a size of 26 nm. Due to this high proportion it is most likely that these particles have had a protein coat of the average size, resulting in the cargo size of 39.2 nm ($26 + 2 \times 6.6$ nm). Thus, our best estimation for the functional diameter of the NPC is 39 nm. This value is in accordance with the diameter of the central pore of the NPC, which has been shown to be ~44 nm in electron microscopy (Hinshaw *et al.*, 1992; Akey and Radermacher, 1993).

These results are in contrast to those of Dworetzky *et al.* (1988), who have previously shown that the *Xenopus* oocyte NPC could import gold particles up to ~23 nm in

diameter, coated with a 1.5-nm-measuring shell of nucleoplasmin. However, the striking difference in the size of the protein coat is most likely a consequence of the different protocols used for coating the gold particles with NP. Whereas Dworetzky *et al.*, (1988) used minimal amount of protein to stabilize gold particles, giving a thin protein layer, we used concentration 10 times higher than the minimal stabilization amount, yielding a larger protein layer.

In addition, the use of saturating amounts of protein had the advantage that the gold particles were fully stabilized so that they could not be modified by nonspecific adsorption of cellular proteins or protein complexes of various sizes upon cell injection, resulting in an unpredictable increase of the protein coat. Furthermore, a fully saturated gold surface ensured that particles can only be transported by the soluble import receptors bound to the NLS of NP and not by adsorption of the receptors to the gold particles.

The soluble import receptors importin α and β were first described in 1994 and 1995 (Görllich *et al.* 1994, 1995; Moroianu *et al.*, 1995; Radu *et al.*, 1995). Thus, the contribution of these receptor proteins that bind to the carrier protein or cargo could not have been considered by Dworetzky in 1988. Therefore, we analyzed the effect of importin α and β on the diameter of cargo-coated gold particles. Our results showed that the protein coat of NP-receptor-coated gold particles is very heterogeneous and has a large variability, resulting in overlapping sizes of just NP and NP- α - β -coated gold. Therefore, it is difficult to define a statistically significant influence of the receptor coat on the diameter of the particles. However, it must be considered that even the contribution of importin α/β to the average diameter of the transported cargo (26-nm gold + 2×8.5 protein layer = 43 nm) would be in agreement with electron microscopically determined diameter of the central pore of the NPC (Hinshaw *et al.*, 1992; Akey and Radermacher, 1993).

It could be argued that some other phenomena have occurred that might have interfered with the import of the cargo-receptor-coated gold particles. First, a dissociation of NP from the gold surface might be assumed. However, it is known that protein adsorption to gold is irreversible (Leunissen and De May, 1989). In addition, the size distribution of the nuclear gold should not show the sharp size limit as has been observed in our experiments. A second concern might be that importin α and/or β might have dissociated from the NP-gold after microinjection. However, both import receptors are known to show an extremely high affinity. Importin α binds to NP with a K_D of ~15 nM and importin β binds to importin α with a K_D of ~40 nM (Catimel *et al.*, 2001).

The central pore of the NPC is often, but not always, plugged with a particle of highly variable appearance (called the central plug or transporter). The existence, definite structure, and functional role of such a particle have been discussed (Panté and Aebi, 1993, 1994; Stoffler *et al.*, 1999). However, all our findings suggest that this plug does not play a functional role in restricting the maximal functional diameter of the nuclear pore.

In addition to providing insights in basic cell research, our findings also have a virological impact. The observation that

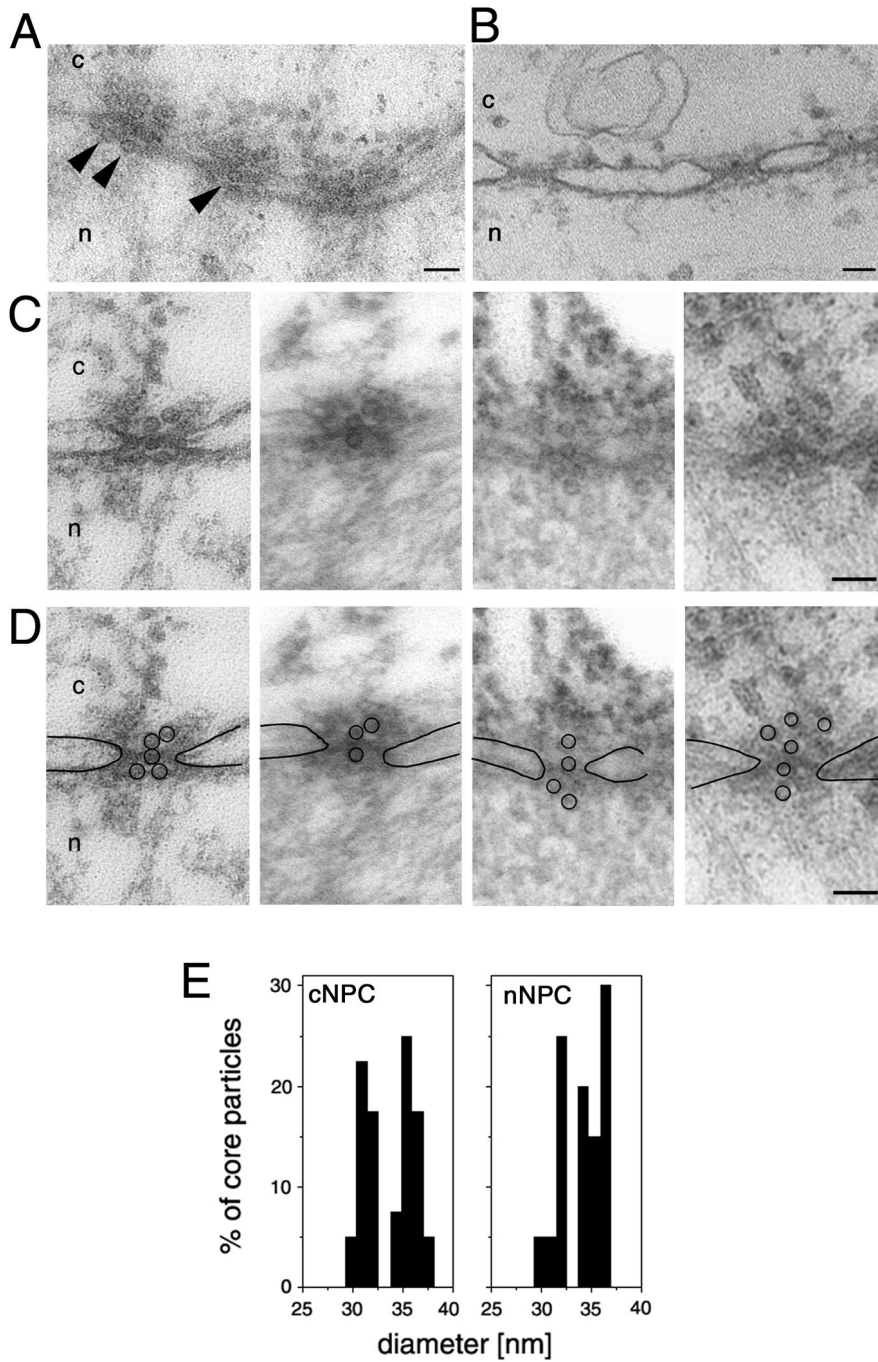


Figure 5. Intact hepatitis B virus cores (32 or 36 nm in diameter) are able to cross the nuclear pores. (A) Views of a nuclear envelope cross section with adjacent cytoplasm (c) and nucleoplasm (n) from a *Xenopus* oocyte that have had phosphorylated recombinant HBV cores microinjected into their cytoplasm. Arrowheads point to core particles associated with the nuclear face of the NPC. (B) Nuclear envelope cross section from a control (noninjected) *Xenopus* oocyte. (C) Examples of cross-sectioned NPCs with associated HBV cores. (D) Same micrographs as in C but with the nuclear membrane boundaries and the HBV cores outlined. (E) Quantitative analysis of the size of core particles associated with the cytoplasmic face of the nuclear pore (cNPC) or the nuclear face of the nuclear pore (nNPC) from oocytes injected with recombinant HBV cores. 60 HBV cores were measured for each histogram. Bars, 100 nm.

intact HBV capsids are found within the nuclear basket suggests a new model for the transport of the HBV genome into the nucleus, which does not require a disassembly at the cytosolic face of the NPC. Our results supported the idea of Kann *et al.* (1999) that the P-cores plugged the NPC, preventing the import of other karyophilic substrates. However, it must be considered that these RNA-containing P-cores reflect the immature HBV capsids and not the mature DNA-containing particles. For the latter population a dis-

sembly must be proposed. Whether this disassembly takes place within the nuclear basket or in the free karyoplasm cannot be answered by the present work. In any case, this finding supports the physiological relevance of our data and additionally shows a strategy that may be used by other viruses or capsids for which a disassembly within the cytosol seemed to be a requirement.

Although significant progress has been made in identification and molecular characterization of the receptor for

the classical NLS pathway (as well as their crystalline structures, which have recently been resolved; reviewed by Chook *et al.*, 1999; Conti and Izaurralde, 2001), very little is known about the precise molecular mechanism for nuclear import of NLS-bearing proteins through the NPC. The knowledge that the NPC is able to transport macromolecules that are close to 40 nm in diameter, instead of 26 nm in diameter, might be a helpful fact for the evaluation of molecular models proposed for translocation through the nuclear pore.

ACKNOWLEDGMENTS

We are most grateful to Ari Helenius for generous support, for making many constructive suggestions, and for critical reading of the manuscript. We thank Dirk Görlich for providing nucleoplasm, importin α and β , and the anti-importin β antibody; and Paul Pumpens and Gallina Borisova (Biomedical Research and Study Center, University of Latvia, Riga, Latvia) for providing the purified *E. coli*-derived core particles. This work was supported by a grant of the Deutsche Forschungsgemeinschaft to M.K. (SFB 535, B5), a grant from the Swiss National Science Foundation to N.P. (3100-053034), and a grant from the Natural Sciences and Engineering Research Council of Canada to N.P.

REFERENCES

- Akey, C.W., and Radermacher, M. (1993). Architecture of the *Xenopus* nuclear pore complex revealed by three-dimensional cryo-electron microscopy. *J. Cell Biol.* 122, 1–19.
- Baschong, W., and Wrigley, N.G. (1990). Small colloidal gold conjugated to Fab fragments or to immunoglobulin G as high-resolution labels for electron microscopy: a technical overview. *J. Electron Microsc. Tech.* 14, 313–323.
- Catimel, B., Teh, T., Fontes, M.R., Jennings, I.G., Jans, D.A., Howlett, G.J., Nice, E.C., and Kobe, B. (2001). Biophysical characterization of interactions involving importin- α during nuclear import. *J. Biol. Chem.* 276, 34189–34198.
- Chook, Y.M., Cingolani, G., Conti, E., Stewart, M., Vetter, I., and Wittinghofer, A. (1999). Pictures in cell biology. Structures of nuclear-transport components. *Trends Cell Biol.* 9, 310–311.
- Cingolani, G., Petosa, C., Weis, K., and Muller, C.W. (1999). Structure of importin- β bound to the IBB domain of importin- α . *Nature* 399, 221–229.
- Conti, E., and Izaurralde, E. (2001). Nucleocytoplasmic transport enters the atomic age. *Curr. Opin. Cell Biol.* 13, 310–319.
- Conti, E., Uy, M., Leighton, L., Blobel, G., and Kuriyan, J. (1998). Crystallographic analysis of the recognition of a nuclear localization signal by the nuclear import factor karyopherin α . *Cell* 94, 193–204.
- Crowther, R.A., Kiselev, N.A., Bottcher, B., Berriman, J.A., Borisova, G.P., Ose, V., and Pumpens, P. (1994). Three-dimensional structure of hepatitis B virus core particles determined by electron cryomicroscopy. *Cell* 77, 943–950.
- De Robertis, E.M., Longthorne, R.F., and Gurdon, J.B. (1978). Intracellular migration of nuclear proteins in *Xenopus* oocytes. *Nature* 272, 254–256.
- Dingwall, C., Sharnick, S.V., and Laskey, R.A. (1982). A polypeptide domain that specifies migration of nucleoplasm into the nucleus. *Cell* 30, 449–458.
- Dworetzky, S.I., Lanford, R.E., and Feldherr, C.M. (1988). The effects of variations in the number and sequence of targeting signals on nuclear uptake. *J. Cell Biol.* 107, 1279–1287.
- Feldherr, C.M., Kallenbach, E., and Schultz, N. (1984). Movement of a karyophilic protein through the nuclear pores of oocytes. *J. Cell Biol.* 99, 2216–2222.
- Frens, G. (1973). Controlled nucleation for the regulation of the particle size in minodisperse gold suspension. *Nature* 241, 20–22.
- Görlich, D., Prehn, S., Laskey, R.A., and Hartmann, E. (1994). Isolation of a protein that is essential for the first step of nuclear import. *Cell* 79, 767–778.
- Görlich, D., Kostka, S., Kraft, R., Dingwall, C., Laskey, R.A., Hartmann, E., and Prehn, S. (1995). Two different subunits of importin cooperate to recognize nuclear localization signals and bind them to the nuclear envelope. *Curr. Biol.* 5, 383–392.
- Hinshaw, J.E., Carragher, B.O., and Milligan, R.A. (1992). Architecture and design of the nuclear pore complex. *Cell* 69, 1133–1141.
- Horisberger, M., and Rosset, J. (1977). Colloidal gold, a useful marker for transmission and scanning electron microscopy. *J. Histochem. Cytochem.* 25, 295–305.
- Kann, M., and Gerlich, W.H. (1994). Effect of core protein phosphorylation by protein kinase C on encapsidation of RNA with core particles of hepatitis B virus. *J. Virol.* 68, 7993–8000.
- Kann, M., Bischof, A., and Gerlich, W.H. (1997). In vitro model for the nuclear transport of the hepadnavirus genome. *J. Virol.* 71, 1310–1316.
- Kann, M., Sodeik, B., Vlachou, A., Gerlich, W.H., and Helenius, A. (1999). Phosphorylation-dependent binding of hepatitis B virus core particles to the nuclear pore complex. *J. Cell Biol.* 145, 45–55.
- Kasamatsu, H., and Nakanishi, A. (1998). How do animal DNA viruses get to the nucleus? *Annu. Rev. Microbiol.* 52, 627–686.
- Kenney, J.M., von Bonsdorff, C.H., Nassal, M., and Fuller, S.D. (1995). Evolutionary conservation in the hepatitis B virus core structure: comparison of human and duck cores. *Structure* 3, 1009–1019.
- Leunissen, J.L., and De May, J.R. (1989). Preparation of gold probes. In *Immuno Gold Labeling*, ed. A.J. Verkleij and J.L. Leunissen, Boca Raton, FL: CRC Press, 3–16.
- Mattaj, I.W., and Englmeier, L. (1998). Nucleocytoplasmic transport the soluble phase. *Annu. Rev. Biochem.* 67, 265–306.
- Moroianu, J., Blobel, G., and Radu, A. (1995). Previously identified protein of uncertain function is karyopherin α and together with karyopherin β docks import substrate at nuclear pore complexes. *Proc. Natl. Acad. Sci. USA* 92, 2008–2011.
- Nakielny, S., and Dreyfuss, G. (1999). Transport of proteins and RNAs in and out of the nucleus. *Cell* 23, 677–690.
- Paine, P.L., Moore, L.C., and Horowitz, S.B. (1975). Nuclear envelope permeability. *Nature* 254, 109–114.
- Panté, N., and Aebi, U. (1993). The nuclear pore complex. *J. Cell Biol.* 122, 977–984.
- Panté, N., and Aebi, U. (1994). Towards understanding the 3-D structure of the nuclear pore complex at the molecular level. *Curr. Opin. Struct. Biol.* 4, 187–196.
- Panté, N., Jarmolowski, A., Izaurralde, E., Sauder, U., Baschong, W., and Mattaj, I.W. (1997). Visualizing nuclear export of different classes of RNA by electron microscopy. *RNA* 3, 498–513.
- Radu, A., Blobel, G., and Moore, M.S. (1995). Identification of a protein complex that is required for nuclear protein import and

mediates docking of import substrate to distinct nucleoporins. *Proc. Natl. Acad. Sci. USA* 92, 1769–1773.

Ribbeck, K., and Görlich, D. (2001). Kinetic analysis of translocation through nuclear pore complexes. *EMBO J.* 20, 1320–1330.

Richardson, W.D., Mills, A.D., Dilworth, S.M., Laskey, R.A., and Dingwall, C. (1988). Nuclear protein migration involves two steps: rapid binding at the nuclear envelope followed by slower translocation through nuclear pores. *Cell* 52, 655–664.

Slot, J.W., and Geuze, H.J. (1985). A new method of preparing gold probes for multiple-labeling cytochemistry. *Eur. J. Cell Biol.* 38, 87–93.

Stoffler, D., Fahrenkrog, B., and Aebi, U. (1999). The nuclear pore complex: from the architecture to functional dynamics. *Curr. Opin. Cell. Biol.* 11, 391–401.

Wente, S.R. (2000). Gatekeepers of the nucleus. *Science* 288, 1374–1377.

Whittaker, G.R., and Helenius, A. (1998). Nuclear import and export of viruses and virus genomes. *Virology* 246, 1–23.

Whittaker, G.R., Kann, M., and Helenius, A. (2000). Viral entry into the nucleus. *Annu. Rev. Cell Dev. Biol.* 16, 627–651.

Wrigley, N.G. (1968). The lattice spacing of crystalline catalase as an internal standard of length in electron microscopy. *J. Ultrastruct. Res.* 24, 454–464.